Anthracene-9,10-diones as Potential Anticancer Agents. Synthesis, DNA-Binding, and Biological Studies on a Series of 2,6-Disubstituted Derivatives

Mavis Agbandje,† Terence C. Jenkins, Robert McKenna,† Anthony P. Reszka, and Stephen Neidle*

Cancer Research Campaign Biomolecular Structure Unit, The Institute of Cancer Research, Sutton, Surrey SM2 5NG, U.K.
Received August 5, 1991

A series of 2,6-bis(ω-aminoalkanamido)anthracene-9,10-diones (9,10-anthraquinones), of general formula Ar-$(NHCO(CH_2)_nNR_2)_2$, where Ar = anthracene-9,10-dione and n = 1 or 2, have been synthesized by treatment of the corresponding bis(ω-haloalkanamido) derivatives with appropriate secondary amines. The DNA-binding properties of these compounds were evaluated by thermal denaturation studies, unwinding of closed-circular DNA, determination of association constants in solution, and examined by molecular modeling. A representative compound in the series has been examined by X-ray crystallography. In vitro cytotoxicity data is reported for the compounds and some indications of structure–activity relationships have been discerned. In particular, those compounds with two methylene links (n = 2) in each side chain separating the amide and terminal amine moieties have superior activity and, in general, enhanced DNA binding characteristics. It is postulated that the mode of reversible binding of these compounds to DNA involves the side chains occupying *both* major and minor grooves and, further, that this may confer cytotoxic properties which are distinct from those of previously reported anthracene-9,10-dione cytotoxins.

Introduction

The aminoalkyl-functionalized anthracene-9,10-dione (9,10-anthraquinone) series of synthetic compounds has been the subject of much study in the quest for more active and less toxic analogues of the anthracycline antitumor antibiotics, daunomycin and adriamycin. Thus, the 1,4-bis derivative mitoxantrone[1,2] has high experimental antitumor activity and has shown some activity in a number of clinical trials[5] particularly against breast cancers and acute leukemias. It is now licensed for clinical use in a number of countries. Its mode of action is believed to involve intercalation into double-helical DNA, as evidenced by unwinding, thermal stabilization, kinetic, and NMR studies.[3,6–10] In common with the anthracyclines themselves, mitoxantrone stimulates the production of double-strand DNA breaks that are mediated by DNA topoisomerase II;[11] it therefore appears likely that intercalation into DNA is a necessary, although by itself insufficient step, to an antitumor effect. Molecular modeling studies[12,13] have confirmed the plausibility of an intercalation model for these agents, in which the substituent groups are in the DNA major groove and the anthracene-9,10-dione chromophore is perpendicular to the base-pair long axis. This model is consistent with kinetic studies,[9,14] which themselves are suggestive of kinetic factors playing a role in the antitumor properties of mitoxantrone.

A number of (amidoalkyl)anthracene-9,10-diones have recently been synthesized, and their DNA-binding and antitumor properties evaluated. Compounds, having substituents at the 1-,[15,16] 2-,[17] 1,4-,[18] and 2,4-positions[19] have been examined. These studies have shown that there are some correlations between cytotoxic activity and position, nature, and length of the side-chain substituents, with a general requirement for $-NHCO(CH_2)_nNR_2$ having n = 2 for significant activity.

The present study extends this work to the 2,6-disubstituted series. Earlier work[12] has suggested that disubstitution at the 1,5-distal positions could result in enhanced cytotoxicity, possibly by virtue of the requirement for the substituents to occupy both major and minor grooves of the DNA double helix, thereby producing kinetically stable complexes.[20] Several of the 2,6-difunctionalized compounds reported in this paper have been examined for antiprotozoal activity;[21] a number of base-functionalized 2,6-bis-ethers of anthracene-9,10-dione have been reported with broad-spectrum antiviral activity.[22]

*Correspondence to this author.
†Present address: Dept. of Biological Sciences, Purdue University, West Lafayette, IN 47907.

(1) Murdock, K. C.; Child, R. C.; Fabio, P. F.; Angier, R. B.; Wallace, R. E.; Durr, F. E.; Citarella, R. V. Antitumor Agents. 1. 1,4-Bis[(aminoalkyl)amino]-9,10-anthracenediones. *J. Med. Chem.* **1979**, *22*, 1024–1030.
(2) Zee-Cheng, R. K.-Y.; Cheng, C. C. Antineoplastic Agents. Structure-Activity Relationship Study of Bis(substituted aminoalkylamino)anthraquinones. *J. Med. Chem.* **1978**, *21*, 291–294.
(3) Lown, J. W., Ed. In *Anthracycline and Anthracenedione-based Anticancer Agents*; Elsevier: Amsterdam, 1988.
(4) Comblect, M. A.; Stuart-Harris, R. C.; Smith, I. E.; Colman, R. E.; Rubers, R. D.; Mouridsen, M. T. Mitoxantrone for the Treatment of Advanced Breast Cancer: Single-agent Therapy in Previously Untreated Patients. *Eur. J. Cancer Clin. Oncol.* **1984**, *20*, 1141–1146.
(5) Stuart-Harris, R. C.; Bozek, T.; Pavlidis, N. A.; Smith, I. E. Mitoxantrone: An Active New Agent in the Treatment of Advanced Breast Cancer. *Cancer Chemother. Pharmacol.* **1984**, *12*, 1–4.
(6) Kapuscinski, J.; Darzynkiewicz, Z. Interactions of Antitumour Agents Ametantrone and Mitoxantrone (Novantrone) with Double-Stranded DNA. *Biochem. Pharmacol.* **1980**, *34*, 4203–4213.
(7) Lown, J. W.; Morgan, A. R.; Yen, S.-F.; Wang, Y.-H.; Wilson, W. D. Characteristics of the Binding of the Anticancer Agents Mitoxantrone and Ametantrone and Related Structures to Deoxyribonucleic Acids. *Biochemistry* **1985**, *24*, 4028–4035.
(8) Rosenberg, L. S.; Carvlin, M. J.; Krugh, T. R. The Antitumour Agent Mitoxantrone Binds Cooperatively to DNA: Evidence for Heterogeneity in DNA Conformation. *Biochemistry* **1986**, *25*, 1002–1008.
(9) Krishnamoorthy, C. R.; Yen, S.-F.; Smith, J. C.; Lown, J. W.; Wilson, W. D. Stopped-Flow Kinetic Analysis of the Interaction of Anthraquinone Anticancer Drugs with Calf Thymus DNA, Poly[d(G-C)]·Poly[d(G-C)], and Poly[d(A-T)]·Poly[d(A-T)]. *Biochemistry* **1986**, *25*, 5933.
(10) Kotovych, G.; Lown, J. W.; Tong, J. P. K. High-Field ^1H and ^{31}P NMR Studies on the Binding of the Anticancer Agent Mitoxantrone to $d[CpGpApTpCpG]_2$. *J. Biomol. Struct. Dyn.* **1986**, *4*, 111–125.
(11) Tewey, K. M.; Rowe, T. C.; Yang, L.; Halligan, B. C.; Liu, L. F. Adriamycin-Induced DNA Damage Mediated by Mammalian DNA Topoisomerase II. *Science* **1984**, 466–468.
(12) Islam, S. A.; Neidle, S.; Gandecha, B. M.; Partridge, M.; Patterson, L. H.; Brown, J. R. Comparative Computer Graphics and Solution Studies of the DNA Interaction of Substituted Anthraquinones based on Doxorubicin and Mitoxantrone. *J. Med. Chem.* **1985**, *28*, 857–864.
(13) Chen, K.-X.; Gresh, N.; Pullman, B. A Theoretical Investigation on the Sequence Selective Binding of Mitoxantrone to Double-Stranded Tetranucleotides. *Nucleic Acids Res.* **1986**, *14*, 3799–3812.

0022-2623/92/1835-1418$03.00/0 © 1992 American Chemical Society

Scheme I. Synthesis of Anthracene-9,10-dione Compounds[a]

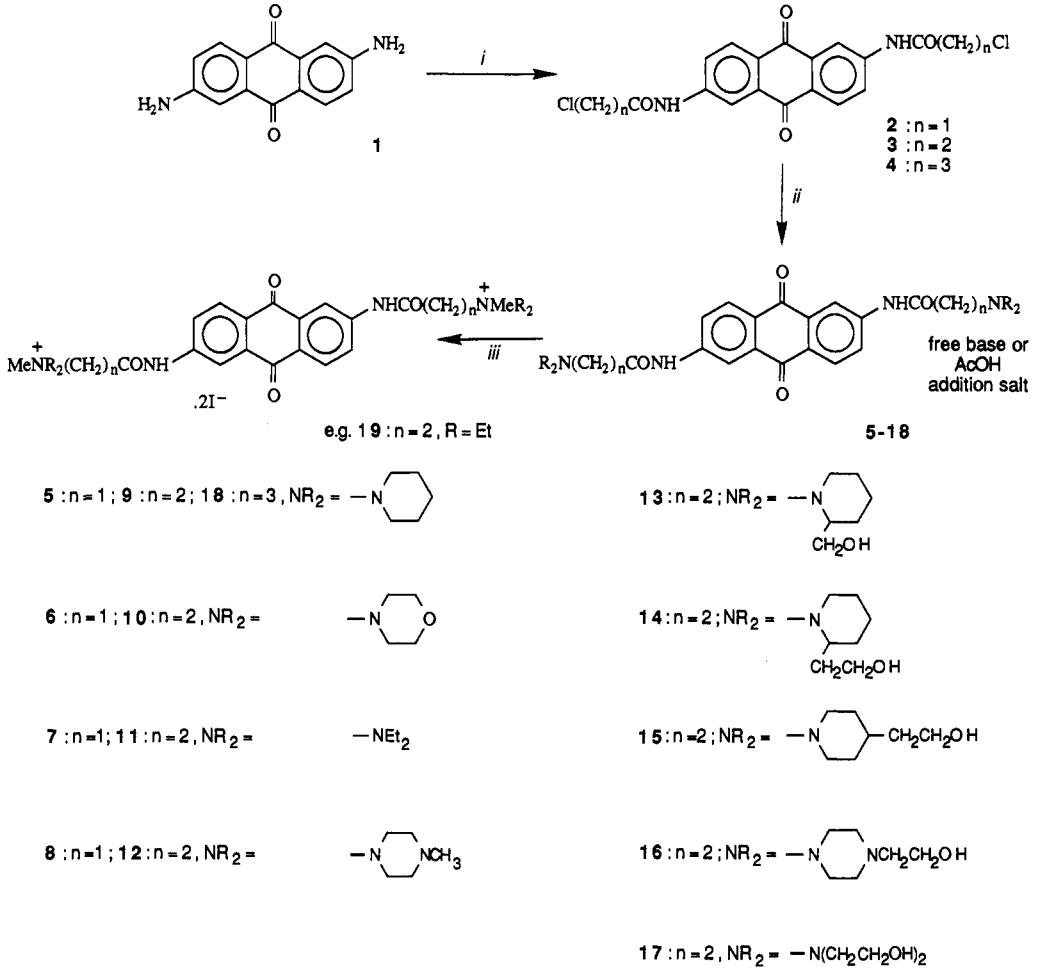

[a] Reagents: (i) excess $Cl(CH_2)_nCOCl$/reflux/3–5 h; (ii) R_2NH/EtOH/reflux/5–23 h followed by treatment with HOAc/heat/30 min for acetic acid addition salts; (iii) excess MeI/acetone/RT/24 h.

This study describes the synthesis of 2,6-bis(ω-aminoalkanamido)anthracene-9,10-diones and the DNA-binding properties of these agents determined both in solution and by molecular modeling. Preliminary biological studies of the cytotoxic behavior of these compounds in leukemic and

Table I. In Vitro Biological Data for Mitoxantrone and the Agents

substance	*n*	estimated pK_a	IC_{50},[a,b] μM L1210	WS	V79
mitoxantrone	–	7.4	0.002	0.01	nd
5	1	10	76.0	>100	30.0
6	1	7.4	>100	>100	>100
7	1	10	27.0	19.0	18.0
8	1	6,9.5	6.50	4.60	4.60
9	2	10.4	0.19	2.00	1.70
10	2	8	0.57	4.20	1.60
11	2	10.8	0.34	2.70	2.90
12	2	9,5	1.70	3.10	1.80
13	2	10	0.50	2.80	3.60
14	2	10	0.28	3.60	12.0
15	2	10	2.30	5.50	3.95
16	2	5,9.5	4.20	6.60	19.5
17	2	9	4.20	>100	25.5

[a] Extracellular concentration required to reduce cell population to 50%. [b] nd = not determined.

(14) Denny, W. A.; Wakelin, L. P. G. Kinetics of the Binding of Mitoxantrone, Ametantrone and Analogues to DNA: Relationship with Binding Mode and Anti-Tumour Activity. *Anti-Cancer Drug Des.* **1990**, *5*, 189–200.

(15) Palumbo, M.; Magno, S. M. Interaction of Deoxyribonucleic Acid with Anthracenedione Derivatives. *Int. J. Biol. Macromol.* **1983**, *5*, 301–307.

(16) Palumbo, M.; Antonello, C.; Viano, I.; Santiano, M.; Gia, O.; Gastaldi, S.; Magno, S. M. New Anthracenedione Derivatives: Interaction with DNA and Biological Effects. *Chem.-Biol. Interactions* **1983**, *44*, 207–218.

(17) Palu, G.; Palumbo, M.; Antonello, C.; Meloni, G. A.; Magno, S. M. A Search for Potential Antitumor Agents: Biological Effects and DNA Binding of a Series of Anthraquinone Derivatives. *Mol. Pharmacol.* **1986**, *29*, 211–217.

(18) Collier, D. A.; Neidle, S. Synthesis, Molecular Modeling, DNA Binding, and Antitumour Properties of Some Substituted Amidoanthraquinones. *J. Med. Chem.* **1988**, *31*, 847–857.

(19) Palumbo, M.; Palu, G.; Gia, O.; Ferrazzi, E.; Gastaldi, S.; Antonello, C.; Meloni, G. A. Bis-Substituted Hydroxy-Anthracenediones: DNA Binding and Biological Activity. *Anti-Cancer Drug Des.* **1987**, *1*, 337–346.

(20) Gandecha, B. M.; Brown, J. R.; Crampton, M. R. Dissociation Kinetics of DNA-Anthracycline and DNA-Anthraquinone Complexes Determined by Stopped-Flow Spectrophotometry. *Biochem. Pharmacol.* **1985**, *34*, 733–736.

(21) Winkelmann, E.; Raether, W. Chemotherapeutically Active Anthraquinones. *Arzneim.-Forsch.* **1979**, *29*, 1504–1509.

(22) Sill, A. D.; Andrews, E. R.; Sweet, F. W.; Hoffman, J. W.; Tiernan, P. L.; Grisar, J. M.; Fleming, R. W.; Mayer, G. D. Bis-Basic-Substituted Polycyclic Aromatic Compounds. A New Class of Antiviral Agents. 5. Bis-Basic Ethers of Anthraquinone and Bisalkamine Esters of Anthraquinonedicarboxylic Acids. *J. Med. Chem.* **1974**, *17*, 965–968.

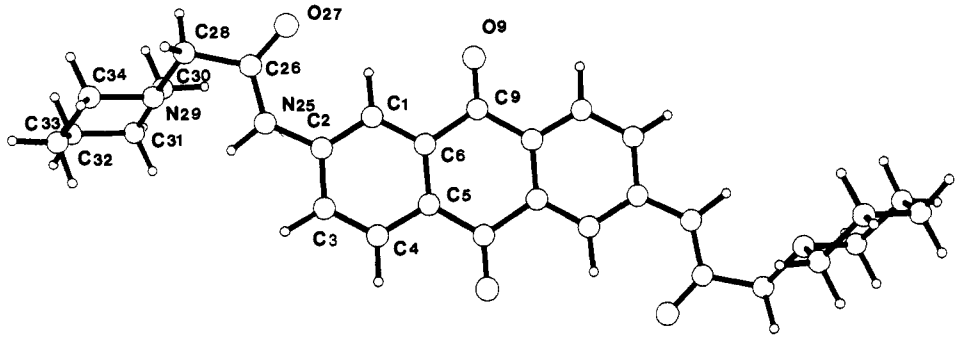

Figure 1. Computer-drawn view of the molecular structure of 2,6-bis(piperidinoacetamido)anthracene-9,10-dione (**5**) as determined by X-ray crystallography.

other cell lines are also provided.

Chemistry

The synthesis of symmetric 2,6-difunctionalized anthracene-9,10-diones **5–17** was accomplished in two steps (Scheme I). The intermediate ω-haloalkanamides **2–4** were prepared in essentially quantitative yield by acylation of diamine **1** with the appropriate (n = 1–3) acid halide. Subsequent aminolysis of **2** and **3** by reflux treatment with the appropriate secondary amines gave the target compounds. This general procedure was successful for compounds with n = 1 or 2, but attempted aminolysis of compounds where n = 3 (e.g. **18**) gave unsatisfactory yields of the required products, even after prolonged reaction times or the addition of catalyst. Attempts to prepare amino-functionalized homologues with n = 3 were abandoned.

Compounds **5–17**, where n = 1 or 2, were obtained in 50–97% yield by means of the scheme outlined; purity was satisfactory, as judged by HPLC, elemental analysis, ^{1}H NMR, and mass spectrometry. Most free-base compounds were only sparingly soluble in water, hence they were converted into their acetic acid addition salts in order to improve the solubility properties. The acetate salts were used for the biophysical and biological studies described below. In addition, the quaternary methiodide salts of several compounds (e.g. **19**) were synthesized. Free bases **13–17**, with side chains containing intrinsic hydroxyl moieties, were of superior aqueous solubility.

Biological Studies in Vitro

Selected compounds in the series were evaluated with L1210 leukemia, Walker 256 (WS) carcinoma, and Chinese hamster V79 cells, with mitoxantrone being used as a control. Results are presented in Table I. Large differences in activity were found, with **5** and **6** having particularly high IC_{50} values; both these have a single methylene group (n = 1) in each side chain. The n = 2 homologues (**9** and **10**), however, have low IC_{50} values for both L1210 and WS cells. Other n = 1 compounds, **7** and **8**, show a similar trend when compared to their n = 2 counterparts (**11** and **12**), albeit at a less extreme level. There is a clear correlation between basicity of the protonatable nitrogen atom(s) in the side chains and the IC_{50} values. Thus, the more basic diethylamino- and piperidino-substituted compounds (**9** and **11**) have the lowest IC_{50} values for both tumor cell lines.

The IC_{50} values for the hydroxyalkyl-substituted piperidine compounds **13–16** are highly dependent on the position of ring substitution, with the 2-substituted isomer **14** having the lowest IC_{50} of this group. Difference between homologues **13** and **14**, of a single methylene group, results in a 2-fold decrease in IC_{50} value. The acyclic bis(2-hydroxyethyl)amino side chain in **17** results in a decreased IC_{50} value for L1210 cells; the IC_{50} value for WS cells is remarkably high, indicating that this compound is unique in the series in producing a (relatively modest) cytotoxic effect in only one of the cell lines examined. In general, compounds in this series showed cytotoxicity in all three cell lines. Only **17** showed marked evidence of a differential cytotoxic effect between tumor and normal cells.

Table II. Crystallographic Data for Compound **5**

formula	$C_{28}H_{32}N_4O_4$
formula weight	244.30
crystal system	orthorhombic
space group	*Pbca*
cell dimensions	a = 16.892 (2) Å
	b = 14.638 (2) Å
	c = 10.616 (4) Å
volume	2625.0 Å^3
μ(Cu Kα)	6.420 cm^{-1}
D_{calc}	1.236 g cm^{-3}
Z, no. of molecules/unit cell	4
F(000)	1040
θ range	1.5–60.0°
max scan time/refln	120 s
no. of unique reflns measured	1947
no. of reflns used	791 with $I \geq 1.0\sigma(I)$
highest peak in final difference map	0.2 e Å^{-3}

Table III. Positional Parameters and Averaged Thermal Parameters,[a] with ESD Values in Parentheses, for Compound **5**

atom	x	y	z	B_{eq}, Å^2
C1	0.8895 (4)	0.3587 (5)	0.5443 (7)	4.6 (2)
C2	0.8799 (4)	0.3225 (5)	0.6647 (7)	4.2 (2)
C3	0.9236 (4)	0.3567 (5)	0.7638 (7)	4.7 (2)
C4	0.9768 (4)	0.4264 (5)	0.7424 (7)	4.3 (2)
C11	0.9882 (4)	0.4631 (5)	0.6238 (6)	4.1 (2)
C12	0.9439 (4)	0.4273 (4)	0.5251 (6)	3.8 (1)
C9	0.9538 (4)	0.4636 (5)	0.3938 (7)	4.8 (2)
O9	0.9168 (3)	0.4311 (4)	0.3062 (5)	7.8 (2)
N25	0.8257 (3)	0.2525 (4)	0.6919 (5)	4.9 (1)
C26	0.7970 (4)	0.1891 (5)	0.6123 (7)	5.3 (2)
O27	0.8115 (3)	0.1858 (4)	0.4986 (5)	7.1 (1)
C28	0.7477 (5)	0.1149 (5)	0.6730 (7)	5.6 (2)
N29	0.7130 (3)	0.1434 (4)	0.7912 (5)	4.6 (1)
C30	0.6429 (5)	0.1999 (5)	0.7684 (8)	6.1 (2)
C31	0.6071 (5)	0.2336 (6)	0.8905 (8)	6.5 (2)
C32	0.5854 (5)	0.1545 (6)	0.9724 (8)	6.8 (2)
C33	0.6562 (5)	0.0934 (6)	0.9935 (8)	7.1 (2)
C34	0.6935 (0)	0.0648 (5)	0.8691 (9)	6.3 (2)

[a] B_{eq}, the average thermal parameter, is defined as: $1.333(a^2B_{11} + b^2B_{22} + c^2B_{33} + bcB_{23}\cos\alpha + acB_{13}\cos\beta + abB_{12}\cos\gamma)$.

Crystallography

The molecular structure of a representative 2,6-disubstituted anthracene-9,10-dione (**5**) was determined by X-ray crystallography in order to obtain geometric and stereochemical information required for the subsequent molecular modeling studies. Crystal quality was poor, so the analysis is not of high accuracy. Views of the structure of **5** are given in Figures 1 and 2. Tables II and III detail

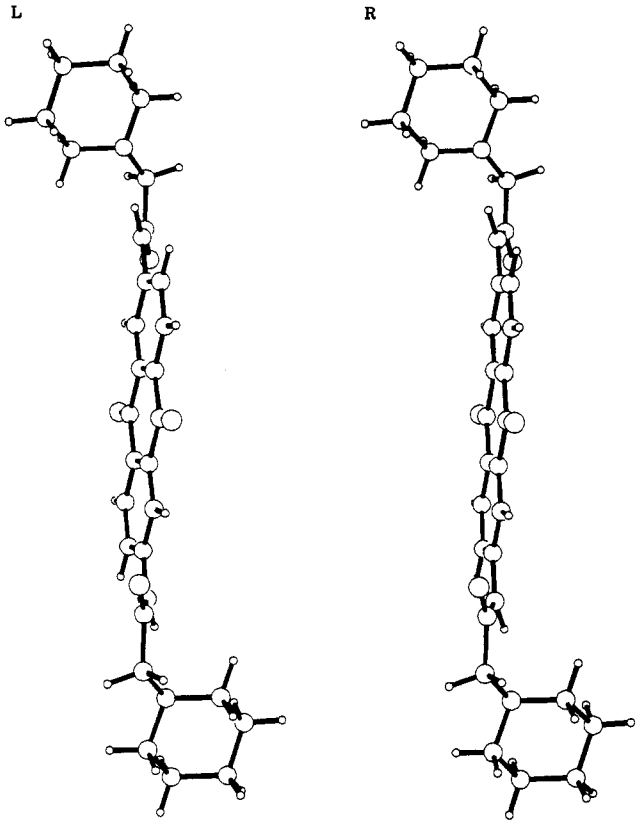

Figure 2. Stereoview of the structure of **5**, viewed along the aromatic plane.

the crystallographic data and atomic coordinates. Calculated values for bond distances and angles are within normal ranges and thus are not discussed here. The molecule has exact 2-fold symmetry in the crystal. The amide groups are oriented so that a carbonyl oxygen atom is cis to its neighboring quinone oxygen atom. The amide group is slightly nonplanar, with a H–N–C–O torsion angle of 173.9°, and is twisted out of the plane of the anthracene chromophore (Figure 2), with a dihedral angle of −26.3°. The chromophore itself is highly coplanar, with the piperidine moiety oriented almost perpendicular to this plane. The N–C–C–N torsion angle involving the amide and piperidine nitrogen atoms is 24°; this cis arrangement results in N···N and N···H nonbonded distances of 2.70 and 2.20 Å, respectively.

DNA Binding in Solution

Several techniques were used to evaluate the DNA-binding properties of compounds **5**–**17**. It was not possible to obtain data for all compounds with every technique due, in part, to solubility/precipitation problems with the employed buffered solutions. Several compounds showed biphasic melting behavior with DNA and hence reliable melting temperatures (T_m) could not be obtained.

The extent to which **5**–**17**, as the derived acetate salts, stabilize the helix-coil thermal denaturation transition of calf thymus DNA is shown in Table IV. All the compounds produced positive ΔT_m values that increased with increasing molar proportion of ligand. At a DNAp to ligand molar ratio of 10:1, thermal denaturation of the complexes formed with **9**, **11**, **14**, **15**, and mitoxantrone are incomplete at temperatures <99 °C, hence the data presented for these agents represent lower-limit values.

There is some variation in ΔT_m values. Thus, the ΔT_m order of **11** > **9** > **12** > **10** is in qualitative agreement with the basicities of the protonatable nitrogen atoms present in the pendant side chains of these agents. There appears

Table IV. Increase in Melting Temperature (ΔT_m) for Calf Thymus DNA on Interaction with Mitoxantrone and the Agents

substance	ΔT_m/°C[a] 40:1	20:1	10:1
mitoxantrone	nd	7.4	≥15.0
5	nd	8.2	14.3
6	0.5	0.5	0.5
7	3.7	7.7	13.5
8	4.2	8.2	13.6
9	3.7	7.3	≥15.3
10	nd	3.0	4.9
11	3.7	7.7	≥15.5
12	nd	4.4	9.2
13	3.8	7.9	14.4
14	4.1	9.2	≥15.3
15	4.3	8.3	≥15.0
16	2.9	4.6	7.2[b]
17	3.2	6.1	10.9[c]

[a] T_m values determined at the DNAp to ligand molar ratios shown; values represent mean from at least three determinations with esd values of ±(0.1–0.3) °C. nd = not determined. [b] ΔT_m at a 5:1 mole ratio was 11.5 ± 0.1 °C. [c] ΔT_m at a 5:1 mole ratio was 14.3 ± 0.1 °C.

Table V. Increases in Melting Temperature (ΔT_m) for Different DNAs on Interaction with Mitroxantrone and the Agents

substance	ΔT_m/°C,[a] CP[b]	CT[c]	ML[d]	possible DNA binding site preference
mitoxantrone	>26.4	≥15.0	>11.7	A/T
5	19.0	14.3	18.4	none
7	16.6	13.5	>16.6	none
9	≥18.9	≥15.3	>14.5	A/T
11	≥20.5	≥15.5	>18.1	none
14	≥18.5	≥15.3	>14.6	A/T
17	11.7	10.9	≥15.7	G/C

[a] Determined at a DNAp to ligand mole ratio of 10:1; values represent mean from at least three determinations with esd values of ±(0.1–0.3) °C. [b] *Clostridium perfringens* DNA (72% [A + T]; T_m for native was 61.1 ± 0.2 °C). [c] Calf thymus DNA (58% [A + T]; T_m for native was 67.0 ± 0.2 °C). [d] *Micrococcus lysodeikticus* DNA (28% [A + T]; T_m for native was 72.0 ± 0.2 °C).

to be only moderate variation with chain length; the diethylamines **7** and **11** and the piperidines **5** and **9**, with n = 1 and n = 2, respectively, produce very similar ΔT_m values in each case. The presence and position of hydroxyl groups within the side chains (cf. **14** and **15**) appears to have only a small effect on ΔT_m values; the behavior of the diethanolamine compound **17** compared to the diethylamine **11** is an exception to this. The ΔT_m values in Table V for DNAs of varying [A + T] versus [G + C] base composition indicate that there are significant differences in base (and possibly sequence) preference between several of the compounds. Thus, **9** and **14** show weak A/T base preference, though less marked than for mitoxantrone, whereas **17** shows a moderate preference for G/C-rich DNA. Compounds **5**, **7**, and **11** have ΔT_m values for the various DNAs that do not vary significantly with [A + T]/[G + C] base composition.

Titration of a number of the compounds (as the derived acetate salts) with calf thymus DNA in aqueous solution and monitoring their absorption spectra showed that hypochromic and bathochromic shifts in the DNA and drug spectra, respectively, were produced as a result of complex formation. Other compounds in the series were insufficiently soluble for reliable data to be obtained. The binding isotherms obtained were highly nonlinear, suggestive of binding site heterogeneity. Binding constants, determined by nonlinear fitting using the extended McGhee–von Hippel equation,[27] are shown in Table VI. All five compounds have a DNA binding site which spans 3–4 base pairs, and the low values of w, the binding co-

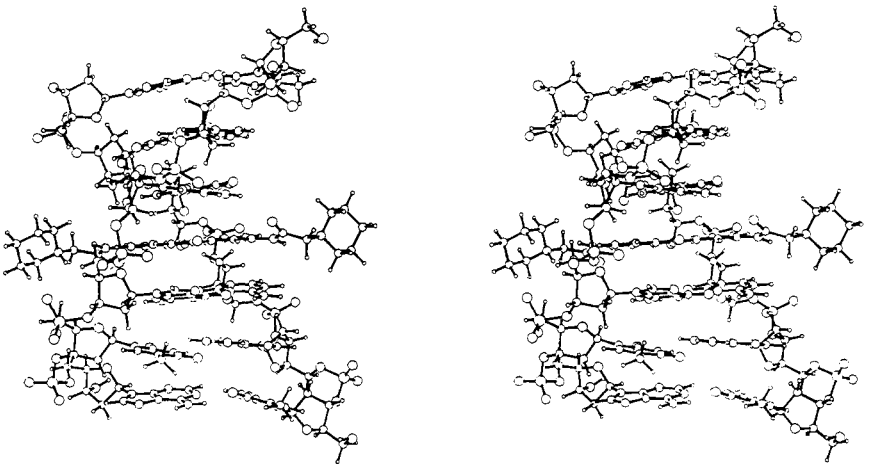

Figure 3. Stereoview of the energy-refined model complex between **5** and the d(TACGTA)$_2$ duplex.

Table VI. (A) DNA-Binding Data for Selected Compounds in the Series and (B) Critical Concentrations (c') and Calculated Unwinding Angles (ϕ) for ccc-pM2 DNA with Ethidium Bromide and Agents in the Series

A

substance	$10^{-6}K$,[a] M^{-1}	n[b]	w[c]
8	20.7	2.830	0.077
9	78.4	3.648	0.229
11	1.39	4.376	0.319
14	0.47	4.100	0.399
17	3.88	4.100	0.228

B

substance	c',[d] μM	ϕ[e]
ethidium bromide	0.8	26°
8	9.7	17°
9	4.0	21°
11	10.4	26°
14	8.7	32°

[a] Calculated using the extended McGhee–von Hippel neighbor-exclusion model. [b] Number of base-pairs occluded by each bound ligand molecule. [c] Cooperativity factor. [d] Concentration at which the ccc-pM2 and "nicked" DNA almost comigrate. [e] Calculated values ±2°.

operativity factor, indicate that the binding is only weakly cooperative.

All compounds examined showed the ability to reverse the supercoiling of PM2 covalently-closed–circular (ccc)-DNA, apart from diethanolamine **17**, which failed to do so even at high concentration (>100 μM). Unwinding angles for **8**, **9**, **11**, and **14** are shown in Table VI.

Molecular Modeling

Interactive molecular graphics was used to visualize plausible low-energy complexes between a number of the compounds (**5**, **7**, **9**, **15**, and **17**) and a hexanucleotide duplex model for intercalated, double-stranded DNA. The graphics was used to optimize potential nonbonded interactions; the resulting structures were then refined by molecular mechanics energy minimization with an all-atom force field to produce calculated binding enthalpies (Table VII).

The starting conformations for the ligands were derived from the crystal structure of **5**, as reported here. The structures of individual molecules, as constructed using the computer graphics, required manual modifications of side-chain conformations compared to that of **5**. This structure is of the free base, with no protonation on the basic nitrogen atoms. As described above, this feature facilitated intramolecular hydrogen bonding with the amide nitrogen atom in the crystal structure, which is not possible when the amine is protonated. Thus, in the case of the N,N′-diprotonated form of **5**, the N–C–C–N torsion angles were altered to transoid conformations.

Table VII. Energies (kcal mol^{-1}) Computed for the Interaction of Agents with the d(CpG) Intercalation Site in d(TACGTA)$_2$

substance	drug–hexamer total energy	drug energy	binding enthalpy: ΔE[a]
5	−310.39	−3.20	−35.34
7	−299.82	1.79	−29.76
9	−324.98	−3.40	−49.73
11	−302.36	4.70	−35.21
15	−331.63	−6.19	−53.59
17	−301.51	9.47	−39.13

[a] Total energy of the energy-refined d(TACGTA)$_2$ B-DNA duplex is −271.85 kcal mol^{-1}. Binding enthalpies were calculated as the total energy of the drug–hexamer complex minus the summed total energies of the separate hexamer and ligand molecules.

It was not possible to produce stereochemically-acceptable models for any of the complexes with the 2- and 6-substituents located simultaneously in either the major or minor groove of the DNA. All plausible arrangements therefore had both grooves occupied simultaneously. In general, arrangements with the anthracene chromophore oriented perpendicular to the long axis of the base pairs were not feasible. Instead, optimal orientations for all compounds examined had an approximately parallel orientation with respect to the base-pair long axis. This resulted in extensive chromophore–base overlaps, with the side-chain components coming close to the sugar–phosphate groups in the grooves, thereby indirectly defining the precise level of overlap for an individual compound.

The low-energy complex formed with **5**, where $n = 1$, has a poor computed binding enthalpy (Table VII). The shortness of the methylene linkages on the side chains precluded extensive nonbonded attractive close contacts between the piperidine rings and the nucleotides in either groove (Figure 3). There are some such contacts between the hydrogen atoms of the piperidine in the minor groove and nucleotide sugar hydrogen atoms on the walls of this groove. Piperidine homologue **9**, with two methylene groups in each side chain, has more extensive contacts in both grooves of the hexamer duplex (Figure 4). This feature is reflected in a significantly higher computed binding enthalpy (Table VII). The acyclic diethylamines **7** and **11** (Figure 5), where $n = 1$ and 2, respectively, similarly show a dependence on chain length for increased side-chain nonbonded attractive interactions with the hexamer duplex, although the difference in calculated enthalpies is smaller. The low-energy complex with **15** (Figure 6 parts a and b) has the side chains extended along

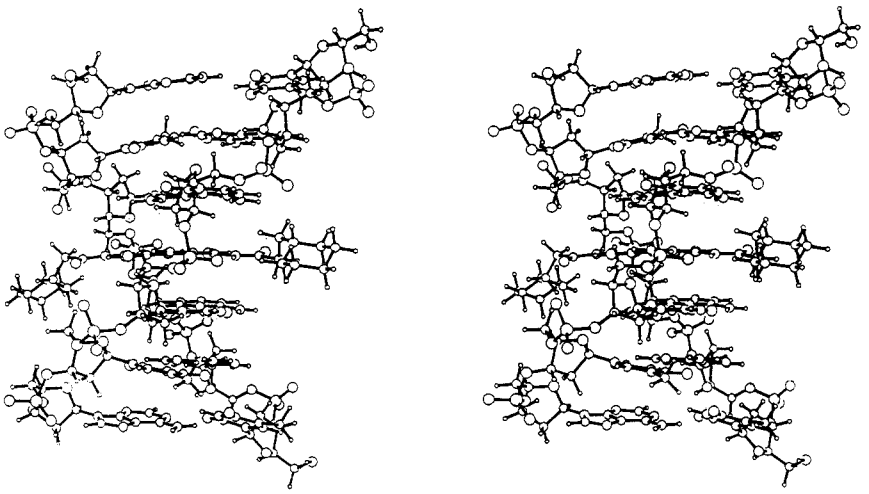

Figure 4. Stereoview of the energy-refined model complex between **9** and the d(TACGTA)$_2$ duplex.

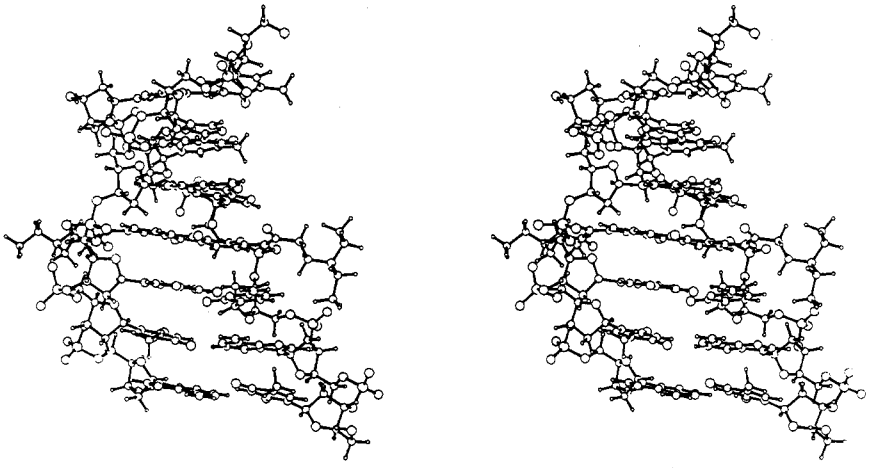

Figure 5. Stereoview of the energy-refined model complex between 11 and the d(TACGTA)$_2$ duplex.

the lengths of both DNA grooves, rather than the more compact arrangement determined as optimal for **9** and 11. The (hydroxyethyl)piperidine rings thus extend to three base-pairs in either direction, with these terminal hydroxyl groups in close, hydrogen-bonded contact with phosphate oxygen atoms; **15** thus has the highest computed binding enthalpy of those examined. The diethanolamine side chains in **17** (Figure 7) have fewer close contacts with the hexanucleotide duplex, resulting in a low calculated binding enthalpy and the terminal hydroxyl groups have minimal influence (cf. 11).

Discussion

This study has shown that 2,6-bis(ω-aminoalkanamido)anthracene-9,10-diones do bind reversibly to double-stranded DNA, as judged by their ability to significantly increase the temperature of the helix-coil transition in DNA. Binding constants for representative compounds are in the normal range for noncovalent DNA-interactive ligands. The variation in values (Table VI) may, in part, be due to binding-site heterogeneity and unavailable data at higher DNAp to ligand ratios. The ability to reverse the unwinding of covalently-closed-circular DNA is characteristic of intercalating ligands.[23] Therefore, we conclude that agents in this series can be generally classed as intercalators. The behavior of **17** is an exception; we are unable to advance any rational explanation for its apparent nonintercalative behavior, particularly since, in accord with other compounds in this series, an acceptable intercalation geometry could be modeled (Table VII).

In general the experimental biophysical data (particularly T_m measurements) indicate that compounds with two methylene groups in the side chains (n = 2) linking chromophore–amide moieties to the positively-charged terminal groups, are stronger DNA binders than those with n = 1. This is in qualitative accord with the computed binding enthalpies for the representative intercalation models examined, with there being significant differences between the **5**,**9** pair. We have previously found that molecular mechanics calculations, following searches for low-energy intercalation structures, can provide useful indicators of binding trends in spite of the many approximations involved,[18,23] such as lack of explicit solvent and the inability to explore all conformational space. The inferior enthalpies computed for the n = 1 derivatives are due in part to decreased stacking interactions between the chromophore and base-pairs at the intercalation site. The shortness of the n = 1 side chains reduces stereochemical flexibility, thus hindering the relief of repulsive contacts with the backbone of the hexanucleotide duplex during docking maneuvres.

The presence of a second methylene group (i.e. n = 2) provides an additional torsion angle which can be maneuvred to remove undesirable steric clashes. The mod-

(23) McKenna, R.; Beveridge, A. J.; Jenkins, T. C.; Neidle, S.; Denny, W. A. Molecular Modelling of DNA-Antitumour Drug Intercalation Interactions: Correlation of Structural and Energetic Features with Biological Properties for a Series of Phenylquinoline-9-carboxamide Compounds. *Mol. Pharmacol.* **1989**, *35*, 720–728.

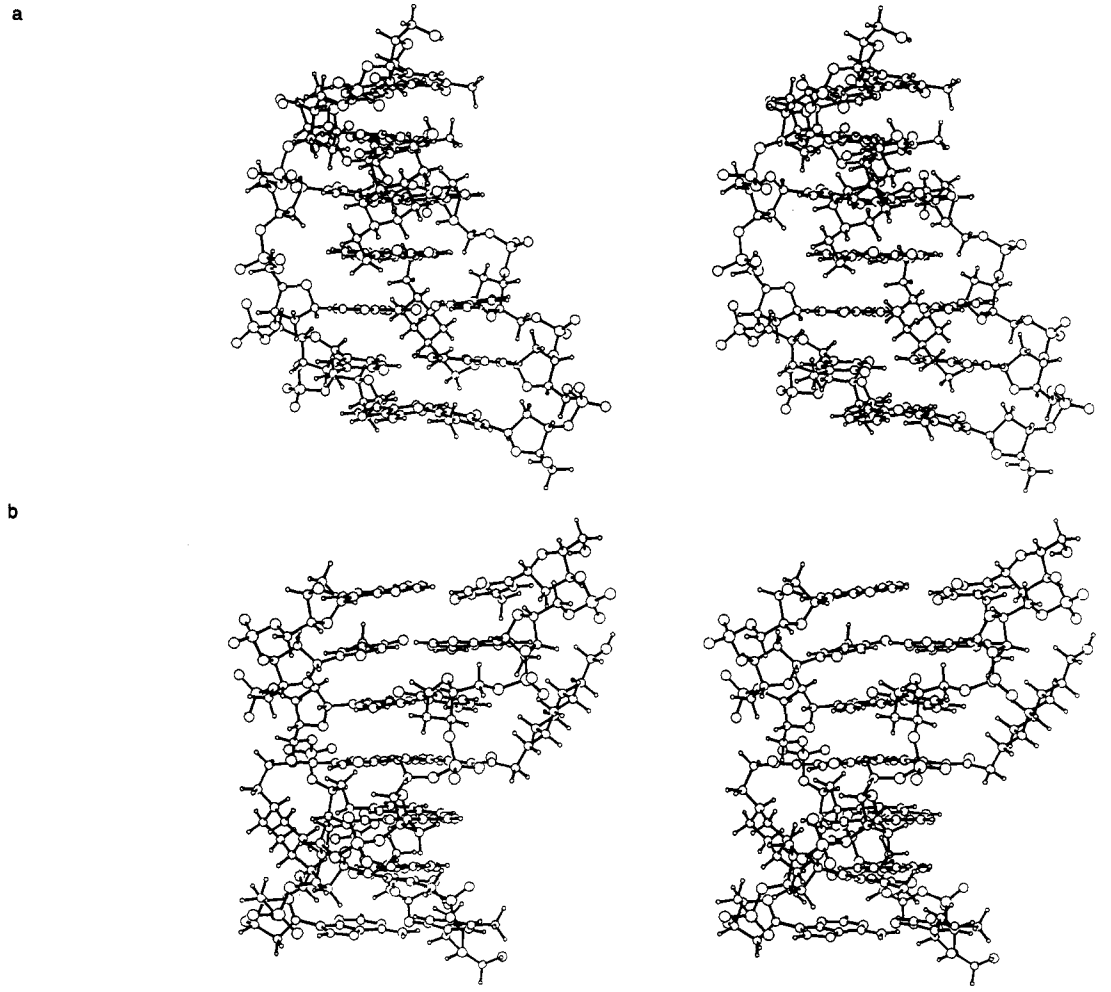

Figure 6. Two stereoviews of the energy-minimized model complex between 15 and the d(TACGTA)$_2$ duplex: (a) viewed toward the major groove, and (b) showing both major and minor grooves.

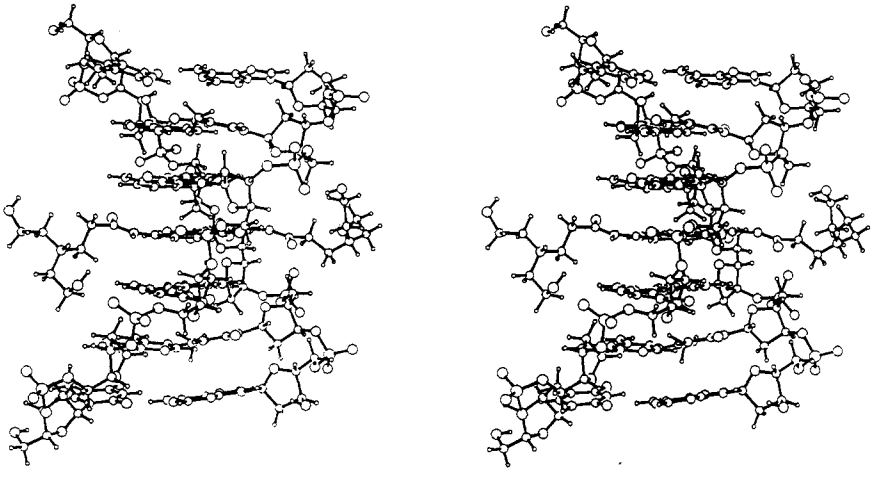

Figure 7. Stereoview of the energy-minimized model complex between 17 and the d(TACGTA)$_2$ duplex.

eling also indicated that compounds with bulky terminal amine substituents gave the largest binding enthalpies, for example, the piperidino derivative **9**. Again, this trend is accord with the experimental binding data. The effect of 4-hydroxyethyl substitution into the piperidine moiety (**15**) is to further increase the calculated binding enthalpy, although the experimental data for this is insufficient to judge if this is a real effect. The predicted decreased interaction of **17** (Table VII), compared to **9** and **15**, is paralleled by its lower ΔT_m values (Table IV). The modeling suggests that this is due to the inability of the diethylamine groups to follow the helical twist of the grooves in as effective a manner as the piperidine moieties, thereby reducing the number of attractive DNA–ligand close contacts. The effectiveness of binding to duplex B-DNA in this series is dependent on the pK_a of the protonatable amine functions. We were unable to incorporate this level of detail in our modeling studies; all modeling was performed on fully-protonated molecules.

The in vitro data with L1210, WS, and V79 cell lines (Table I) provide further evidence of the requirement for two methylene groups in the side chain, since **5–7** are less active than their $n = 2$ homologues. Optimal activity in both tumor cell lines was shown by both the acyclic (**11**)

and cyclic amine moieties (9, 13, and 14). This data can be taken as supporting the hypothesis that DNA-binding is implicated in the cytotoxic effects shown by these compounds. However, detailed correlations with the biophysical data are probably unjustified; cf. the reduced activity apparent when the hydroxyethyl substituent is at the 4-position (15 and 16). The cytotoxic activity of all compounds examined is modest compared to mitoxantrone itself, in accord with the reduced activity shown by 1,4-disubstituted anthracene-9,10-diones.[18] Preliminary in vivo studies with experimental tumors on selected compounds in the present series (Agbandje, Jenkins, and Neidle, unpublished observations) indicate activity in the L1210 leukaemia BDF/1 mouse model for 15 and 16, at ip dose levels of 200 and 100 mg kg^{-1}, respectively, with an ILS of ca. 37% in each case. Further, plasma stability studies by HPLC revealed that 15 and 16 are not degraded following incubation for 2 h at 37 °C.

The particular pattern of side-chain substitution in this series, at the 2,6-distal positions, was chosen since it would be predicted to intercalate in duplex DNA with both major and minor grooves being occupied simultaneously, possibly resulting in slow association and dissociation kinetics for the complex. This hypothesis has been verified by kinetic studies on calf thymus DNA and synthetic polynucleotides which have revealed behavior typical for a DNA-threading molecule (Wilson, Agbandje, Jenkins, and Neidle, to be published). We have shown here that these compounds do indeed bind intercalatively to double-stranded DNA. The threading mode of DNA binding may be related to their weak mutagenicity in Ames-type tests and concentrations compared to mitoxantrone and other anthraquinone-based antitumour compounds (Venitt, Crofton-Sleigh, Agbandje, Jenkins, and Neidle, to be published). This provides an impetus for the further development of compounds in this series with piperidine and piperazine functionalized derivatives where n = 2, e.g. 15 and 16.

Experimental Section

Synthetic Chemistry. NMR spectra were obtained at 250 MHz (Me_2SO-d_6, 20 ± 1 °C) with a Bruker AC250 spectrometer using Me_4Si as internal standard. A Perkin-Elmer 1720X-FT instrument furnished the IR spectra. Mass spectra were obtained with a VG7070H spectrometer (115–150 °C source temperature) using EI (70 eV) or FAB ionization. Melting points are uncorrected. Elemental analyses were carried out by Butterworths Laboratories Ltd., Middlesex, UK; results for elements indicated by symbols were within ±0.3% of the theoretical values. *N,N*-Dimethylformamide (DMF) was distilled under reduced pressure from molecular sieves before use. Ether refers to sodium-dried diethyl ether. TLC was carried out with silica gel (Merck 60F-254) using EtOH as eluent, with visualization at 254 nm and/or by I_2 staining. Column chromatography was accomplished with silica gel (Merck 60, 70-230 ASTM). Solvents were evaporated under reduced pressure.

2,6-Bis(3-chloropropionamido)anthracene-9,10-dione (3). General Acylation Procedure. A suspension of 2,6-diaminoanthracene-9,10-dione (1; 30.0 g, 126 mmol) in freshly-distilled 3-chloropropanoyl chloride (500 g, 3.94 mol) was refluxed for 5 h, until TLC indicated completion of reaction. After cooling to 0–5 °C, the mixture was filtered and the solids were washed with ether (4 × 100 mL) and 1,4-dioxane (2 × 400 mL). Recrystallization from DMF–EtOH (4:1 v/v) afforded propionamide 3 (51.5 g, 95%) as orange crystals: mp >340 °C; IR (KBr) 3372 (NH), 3245, 3170, 1703 (C=O), 1657 (quinone C=O), and 1582 cm^{-1}; NMR δ 2.93 (t, J = 6.2 Hz, 4 H, $COCH_2$), 3.92 (t, J = 6.2 Hz, 4 H, CH_2Cl), 8.07 (dd, J = 1.8 Hz, J = 8.5 Hz, 2 H, H-3,7), 8.16 (d, J = 8.5 Hz, 2 H, H-4,8), 8.44 (d, J = 1.8 Hz, 2 H, H-1,5), and 10.77 (s, 2 H, D_2O removes, NH). Anal. ($C_{20}H_{16}N_2O_4Cl_2$) C, H, N, Cl.

2,6-Bis(2-chloroacetamido)anthracene-9,10-dione (2). Diaminoquinone 1 was treated with chloroacetyl chloride generally according to the method for the preparation of 3 above, except that reflux was for only 3 h and the recrystallization solvent was EtOH, to give chloro amide 2 (91%) as yellow prisms: mp 310–311 °C; IR (Nujol) 3370 (NH), 3335, 3300, 1722 (C=O), 1685 (quinone C=O), and 1590 cm^{-1}; NMR δ 4.35 (s, 4 H, CH_2Cl), 8.07 (dd, J = 8.5 Hz, J = 2.1 Hz, 2 H, H-3,7), 8.20 (d, J = 8.5 Hz, 2 H, H-4,8), 8.44 (d, J = 2.1 Hz, 2 H, H-1,5), and 10.90 (s, 2 H, D_2O removes, NH). Anal. ($C_{18}H_{12}N_2O_4Cl_2$) C, H, N, Cl.

2,6-Bis(4-chlorobutyramido)anthracene-9,10-dione (4). Compound 1 was treated with excess 4-chlorobutanoyl chloride generally according to the method for the preparation of 3 above, except that a catalytic amount of pyridine (0.1 mol equiv) was added and reflux was for only 4 h, to give butyramide 4 in almost quantitative yield. Recrystallization from DMF–EtOH (4:1 v/v) furnished an orange solid: mp >340 °C; IR (Nujol) 3350 (NH), 3300, 3240, 3175, 3110, 1706 (C=O), 1660 (quinone C=O), and 1575 cm^{-1}; NMR δ 2.07 (quint, J = ca. 7 Hz, 4 H, $CH_2CH_2CH_2$), 2.59 (t, J = 7.2 Hz, 4 H, $COCH_2$), 3.73 (t, J = 6.5 Hz, 4 H, CH_2Cl), 8.06 (dd, J = 8.5 Hz, J = 1.8 Hz, 2 H, H-3,7), 8.15 (d, J = 8.5 Hz, 2 H, H-4,8), 8.44 (d, J = 1.8 Hz, 2 H, H-1,5), and 10.66 (s, 2 H, D_2O removes, NH). Anal. ($C_{22}H_{20}N_2O_4Cl_2$) C, H, N, Cl.

2,6-Bis(piperidinoacetamido)anthracene-9,10-dione (5). General Aminolysis Procedure. Piperidine (30 mL, 0.30 mol) was added during 15 min to a stirred, refluxing suspension of chloroacetamide 2 (10.0 g, 25.6 mmol) in EtOH (300 mL). After 5 h of reflux, at which time the reaction was judged (TLC) to have reached completion, the solution was chilled to 0–5 °C. The solid which separated was removed by filtration, washed thoroughly with ether, digested in $CHCl_3$ (150 mL), and treated with decolorizing charcoal (500 mg). Filtration and evaporation gave an amorphous brown powder. Recrystallization from $CHCl_3$–EtOH (3:2 v/v) afforded 5 (7.73 g, 62%) as yellow-green prisms: mp 235–236 °C; IR (Nujol) 3295 (NH), 3200 (br), 3100, 3055, 1700 (C=O), 1673 (quinone C=O), 1600, and 1580 cm^{-1}; NMR δ 1.30–1.42 (m, 4 H, $N(CH_2)_2CH_2$), 1.55–1.58 (m, 8 H, NCH_2CH_2), 2.46–2.50 (m, 8 H, NCH_2CH_2), 3.16 (s, 4 H, $COCH_2$), 8.14 (dd, J = 8.0 Hz, J = 2.1 Hz, 2 H, H-3,7), 8.17 (d, J = 8.0 Hz, 2 H, H-4,8), 8.54 (d, J = 2.1 Hz, 2 H, H-1,5) and 10.39 (s, 2 H, D_2O removes, NH); MS (rel intensity) m/z 488 ($[M]^{\cdot+}$, 4), 405 ($[M - C_5H_{10}N]^{\cdot+}$, 6), 98 ($[C_7H_{12}N]^{\bullet+}$, 100), and 84 ($[C_5H_{10}N]^{\cdot+}$, 35). Anal. ($C_{28}H_{32}N_4O_4$) C, H, N. Diacetate salt: mp 210–212 °C. Dimethiodide: mp 245–247 °C dec.

2,6-Bis(morpholinoacetamido)anthracene-9,10-dione (6). Treatment of compound 2 with excess morpholine, according to the general aminolysis procedure for 5 above, except that boiling was continued for 7 h and the recrystallization solvent was EtOH–$CHCl_3$ (1:1 v/v), afforded acetamide 6 (64%) as yellow prisms: mp 263–264 °C; IR (Nujol) 3285 (NH), 3115, 3080, 1687 (C=O), 1669 (quinone C=O), and 1592 cm^{-1}; NMR δ 2.53 (s, 8 H, NCH_2CH_2), 3.23 (s, 4 H, $COCH_2$), 3.46 (m, 8 H, NCH_2CH_2), 8.16 (s, 4 H, H-3,4,7,8), 8.52 (s, 2 H, H-1,5), and 10.45 (s, D_2O removes, 2 H, NH); MS (rel intensity) m/z 492 ($[M]^{\cdot+}$, 2), 406 ($[M - C_4H_8NO]^{\cdot+}$, 1), 368 (5), 236 (3), 100 ($[C_5H_{10}NO]^{\bullet+}$, 100), 86 ($[C_4H_8NO]^{\bullet+}$, 14) and 83 (20). Anal. ($C_{26}H_{28}N_4O_6$) C, H, N. Diacetate salt: 262–263 °C. Dimethiodide: 244–246 °C dec.

2,6-Bis[(diethylamino)acetamido]anthracene-9,10-dione (7). Acetamide 2 was treated with excess diethylamine according to the general aminolysis procedure used for 5 above, to give amide 7 (62%), after recrystallization from EtOH, as green plates: mp 191–192 °C; IR (Nujol) 3235 (NH), 3090, 1680 (C=O), 1662 (quinone C=O), and 1594 cm^{-1}; NMR δ 1.03 (t, J = 7.1 Hz, 12 H, NCH_2CH_3), 2.63 (q, J = 7.1 Hz, 8 H, NCH_2CH_3), 3.26 (s, 4 H, $COCH_2$), 8.18 (s, 4 H, H-3,4,7,8), 8.56 (s, 2 H, H-1,5), and 10.35 (s, D_2O removes, 2 H, NH); MS (rel intensity) m/z 464 ($[M]^{\bullet+}$, 2), 449 (2), 436 ($[M - C_2H_4]^{\bullet+}$, 1), 393 (2), 378 ($[M - C_5H_{12}N]^{\cdot+}$, 1), 86 ($[C_5H_{12}N]^{\bullet+}$, 100), and 28 ($[C_2H_4]^{\cdot+}$, 100). Anal. ($C_{28}H_{32}N_4O_4$) H, N; C: calcd, 67.22; found, 67.81. Diacetate salt: mp 188–189 °C. Anal. ($C_{30}H_{40}N_4O_8$) C, H, N. Dimethiodide: mp 240–241.5 °C dec.

2,6-Bis[(4-methylpiperazino)acetamido]anthracene-9,10-dione (8). Reflux treatment of chloroamide 2 with 4-methylpiperazine, according to the general aminolysis procedure, gave acetamide 8 (55%), after recrystallization from $CHCl_3$–ether (1:2 v/v), as brown-yellow prisms: mp 213.5–214 °C; IR (Nujol) 3345 (NH), 3260, 3180, 1718 (C=O), 1660 (quinone C=O), and 1578 cm^{-1}; NMR δ 2.17 (s, 6 H, NCH_3), 2.38 (m, 8 H, $COCH_2NCH_2CH_2$), 2.50 (m, 8 H, CH_2NCH_3), 3.19 (s, 4 H, $COCH_2$), 8.11 (dd, J = 8.6

Hz, J = 2.0 Hz, 2 H, H-3,7), 8.17 (d, J = 8.6 Hz, 2 H, H-4,8), 8.50 (d, J = 2.0 Hz, 2 H, H-1,5), and 10.39 (s, D_2O removes, 2 H, N*H*); MS (rel intensity) m/z 518 ($[M]^{\cdot+}$, 49), 405 ($[M - C_6H_{13}N_2]^{\cdot+}$, 6), 368 (20), 236 (6), 113 ($[C_6H_{13}N_2]^{\cdot+}$, 100), and 98 ($[C_6H_{13}N_2 - 1]^{\cdot+}$, 28). Anal. ($C_{28}H_{34}N_6O_4$) C, H, N. Tetraacetate salt: mp 215–217.5 °C. Anal. ($C_{36}H_{50}N_6O_{12}$) C, H, N. Tetramethiodide: mp 268.5–270 °C dec.

2,6-Bis(3-piperidinopropionamido)anthracene-9,10-dione (9). Treatment of chloroamide **3** with piperidine according to the general method for the preparation of **5** above, except that the recrystallization solvent was DMF–EtOH (10:1 v/v), afforded amide **9** (96%) as yellow-brown microcrystals: mp 270–271 °C; IR (Nujol) 3325 (NH), 3290, 3190, 3115, 1700 (C=O), 1672 (quinone C=O), 1618, and 1590 cm^{-1}; NMR δ 1.39 (m, 4 H, $(CH_2)_2CH_2(CH_2)_2$), 1.49 (m, 8 H, $NCH_2CH_2CH_2$), 2.38 (m, 8 H, $N(CH_2CH_2)_2CH_2$), 2.45–2.70 (m, 8 H, $COCH_2CH_2N$), 8.05 (dd, J = 8.8 Hz, J = 2.0 Hz, 2 H, H-3,7), 8.17 (d, J = 8.8 Hz, 2 H, H-4,8), 8.42 (d, J = 2.0 Hz, 2 H, H-1,5), and 10.84 (s, D_2O removes, 2 H, N*H*); MS (rel intensity) m/z 516 ($[M]^{\cdot+}$, 4), 431 ($[M - C_5H_{10}N - 1]^{\cdot+}$, 10), 346 (63), 318 (10), 292 (37), 238 (30), 112 ($[C_7H_{14}N]^{\cdot+}$, 4), 98 ($[C_6H_{12}N]^{\cdot+}$, 40), 84 ($[C_5H_{10}N]^{\cdot+}$, 56), and 83 (90). Anal. ($C_{30}H_{36}N_4O_4$) C, H, N. Diacetate salt: mp 244–246 °C dec. Anal. ($C_{34}H_{44}N_4O_8$) C, H, N. Dimethiodide: mp 262–264.5 °C dec.

2,6-Bis(3-morpholinopropionamido)anthracene-9,10-dione (10). Treatment of compound **3** with morpholine generally according to the aminolysis procedure for **5** above, except that reflux was required for 17 h and the recrystallization solvent was DMF–EtOH (4:1 v/v), gave amide **10** (83%) as a yellow-brown powder: mp 270.5–271.5 °C; IR (Nujol) 3325 (NH), 3290, 3195, 3120, 1698 (C=O), 1670 (quinone C=O), 1613, and 1589 cm^{-1}; NMR δ 2.42 (t, J = 4.5 Hz, 8 H, $N(CH_2CH_2)_2O$), 2.55–2.68 (ABq, 8 H, $COCH_2CH_2$), 3.57 (t, J = 4.5 Hz, 8 H, $N(CH_2CH_2)_2O$), 8.07 (dd, J = 8.6 Hz, J = 2.0 Hz, 2 H, H-3,7), 8.17 (d, J = 8.6 Hz, 2 H, H-4,8), 8.44 (d, J = 2.0 Hz, 2 H, H-1,5), and 10.70 (s, D_2O removes, 2 H, N*H*); MS (rel intensity) m/z 520 ($[M]^{\cdot+}$, 2), 433 ($[M + 1 - C_4H_8NO]^{\cdot+}$, 3), 346 (52), 292 (29), 238 (30), 100 ($[C_5H_{10}NO]^{\cdot+}$, 37), and 86 ($[C_4H_8NO]^{\cdot+}$, 100). Anal. ($C_{28}H_{32}N_4O_6$) C, H, N. Diacetate salt: mp 255–257 °C. Dimethiodide: mp 232–233 °C.

2,6-Bis[3-(diethylamino)propionamido]anthracene-9,10-dione (11). Chloroamide **3** was treated with diethylamine according to the general aminolysis procedure. Recrystallization from DMF–EtOH (4:1 v/v) furnished amino amide **11** (88%) as bright yellow prisms: mp 200–201 °C; IR (KBr) 3315 (NH), 3280, 3185, 3110, 3055, 1698 (C=O), 1669 (quinone C=O), 1611, and 1586 cm^{-1}; NMR δ 0.98 (t, J = 7.1 Hz, 12 H, CH_2CH_3), 2.50 (qt, J = 7.1 Hz, J = 6.9 Hz, 12 H, CH_2CH_3 and $COCH_2$), 2.77 (t, J = 6.9 Hz, 4 H, $COCH_2CH_2$), 8.05 (dd, J = 8.5 Hz, J = 2.0 Hz, 2 H, H-3,7), 8.16 (d, J = 8.5 Hz, 2 H, H-4,8), 8.42 (d, J = 2.0 Hz, 2 H, H-1,5), and 10.75 (s, D_2O removes, 2 H, N*H*); MS (rel intensity) m/z 493 ($[M + 1]^{\cdot+}$, 100), 492 ($[M]^{\cdot+}$, 29), 461 (29), 369 (80), 364 ($[M - C_7H_{14}NO]^{\cdot+}$, 14), 277 (100), 186 (100), 185 (100), and 82 (26). Anal. ($C_{28}H_{36}N_4O_4$) H, N; C: calcd, 68.27; found, 67.72. Diacetate salt: mp 201–203 °C dec. Dimethiodide: mp 242.5–243.5 °C. Anal. ($C_{30}H_{42}N_4O_4I_2$) C, H, N; I: calcd, 32.69; found, 32.03.

2,6-Bis[3-(4-methylpiperazino)propionamido]anthracene-9,10-dione (12). Propionamide **3** was treated with 4-methylpiperazine generally according to the method for the preparation of **5** above, except that reflux was for 9 h and the recrystallization solvent was dry DMF, to give **12** in almost quantitative yield as a green-yellow powder: mp 281–282 °C; IR (KBr) 3340 (NH), 3300, 3105, 3060, 1699 (C=O), 1662 (quinone C=O), 1617, and 1580 cm^{-1}; NMR δ 2.14 (s, 6 H, NCH_3), 2.3–2.7 (m, 24 H, aliph-H), 8.00 (dd, J = 8.5 Hz, J = 2.1 Hz, 2 H, H-3,7), 8.17 (d, J = 8.5 Hz, 2 H, H-4,8), 8.43 (d, J = 2.1 Hz, 2 H, H-1,5), and 10.76 (s, D_2O removes, 2 H, N*H*); MS (rel intensity) m/z 547 ($[M + 1]^{\cdot+}$, 100), 546 ($[M]^{\cdot+}$, 31), 461 (3), 369 (100), 364 (100), 448 ($[M + 1 - C_5H_{11}N_2]^{\cdot+}$, 17), 447 ($[M - C_5H_{11}N_2]^{\cdot+}$, 17), 369 (100), and 364 (55). Anal. ($C_{30}H_{38}N_6O_4 \cdot 1.5H_2O$) C, H, N. Tetraacetate salt: mp 207–209 °C.

2,6-Bis[3-[2-(hydroxymethyl)piperidino]propionamido]anthracene-9,10-dione (13). Treatment of chloroamide **3** with 2-(hydroxymethyl)piperidine according to the general aminolysis procedure, except that reflux was for 23 h and the crude product was digested in dry DMF prior to treatment with charcoal. Trituration of the filtrate with dry ether gave amide **13** (86%) as yellow prisms: mp 216–217 °C dec; IR (Nujol) 3440 (br, OH), 3300 (br, NH), 3200, 3120, 3060, 1700 (C=O), 1672 (quinone C=O), 1613, and 1589 cm^{-1}; NMR δ 1.1–1.8 (m, 12 H, $NCH_2(CH_2)_3$), 2.1–2.3 (m, 4 H, $NCH_2(CH_2)_3$), 2.5–2.9 (ABm, 8 H, $COCH_2CH_2$), 3.11 (m, 2 H, $CHCH_2$), 3.47 (m, 4 H, CH_2OH), 4.48 (s, D_2O removes, 2 H, O*H*), 8.05 (dd, J = 8.5 Hz, J = 2.1 Hz, 2 H, H-3,7), 8.16 (d, J = 8.5 Hz, 2 H, H-4,8), 8.44 (d, J = 2.1 Hz, 2 H, H-1,5), 10.86 (s, D_2O removes, 2 H, N*H*); MS (rel intensity) m/z 577 ($[M + 1]^{\cdot+}$, 28), 545 ($[M - CH_3O]^{\cdot+}$, 8), 462 ($[M - C_6H_{12}NO]^{\cdot+}$, 2), 407 ($[M + 1 - C_9H_{18}NO_2]^{\cdot+}$, 2), 369 (2), 277 (13), 185 ($[C_6H_{17}N_2O]^{\cdot+}$, 100), 168 ($[C_9H_{18}NO_2 - 2]^{\cdot+}$, 22), 128 ($[C_7H_{14}NO]^{\cdot+}$, 100), and 114 ($[C_6H_{12}NO]^{\cdot+}$, 72). Anal. ($C_{32}H_{40}N_4O_6 \cdot 0.5H_2O$) C, H, N. Diacetate salt: mp 179–180 °C.

2,6-Bis[3-[2-(2-hydroxyethyl)piperidino]propionamido]anthracene-9,10-dione (14). Propionamide **3** was treated with 2-(2-hydroxyethyl)piperidine according to the general aminolysis procedure, except that boiling was for 16 h and the crude product was digested in dry DMF prior to treatment with decolorizing charcoal. Trituration with acetone and chilling gave amino amide **14** (50%) as an amorphous brown solid: mp 211–212 °C; IR (KBr) 3400 (br, OH), 3300 (br, NH), 3180, 3106, 3050, 1695 (C=O), 1668 (quinone C=O), 1606, and 1584 cm^{-1}; NMR δ 1.28 (m, 4 H, $N(CH_2)_2CH_2$), 1.4–1.9 (m, 12 H, CH_2CH_2OH and $NCH_2CH_2CH_2CH_2$), 2.25–2.32 (m, 4 H, $COCH_2$), 2.50–2.54 (m, 4 H, $NCH_2(CH_2)_2$), 2.64–2.80 (m, 4 H, $COCH_2CH_2$), 2.89–2.97 (m, 2 H, $NCH(CH_2)_2$), 3.40–3.49 (m, 4 H, CH_2OH), 4.44 (s, D_2O removes, 2 H, O*H*), 8.07 (dd, J = 8.5 Hz, J = 2.1 Hz, 2 H, H-3,7), 8.17 (d, J = 8.5 Hz, 2 H, H-4,8), 8.42 (d, J = 2.1 Hz, 2 H, H-1,5), and 10.80 (s, D_2O removes, 2 H, N*H*); MS (rel intensity) m/z 605 ($[M + 1]^{\cdot+}$, 100), 604 ($[M]^{\cdot+}$, 26), 588 ($[M + 1 - OH]^{\cdot+}$, 22), 577 ($[M + 1 - C_2H_4]^{\cdot+}$, 11), 576 ($[M - C_2H_4]^{\cdot+}$, 10), 560 ($[M + 1 - C_2H_5O]^{\cdot+}$, 20), 559 ($[M - C_2H_5O]^{\cdot+}$, 15), 448 ($[M - C_9H_{18}NO]^{\cdot+}$, 20), 421 ($[M + 1 - C_{10}H_{18}NO_2]^{\cdot+}$, 21), 420 ($[M - C_{10}H_{18}NO_2]^{\cdot+}$, 14), 406 ($[M + 1 - C_{10}H_{19}N_2O_2]^{\cdot+}$, 18), and 405 ($[M - C_{10}H_{18}N_2O_2]^{\cdot+}$, 18). Anal. ($C_{34}H_{44}N_4O_6 \cdot 0.5H_2O$) C, H, N. Diacetate salt: mp 178–179 °C.

2,6-Bis[3-[4-(2-hydroxyethyl)piperidino]propionamido]anthracene-9,10-dione (15). Treatment of chloro amide **3** with 4-(2-hydroxyethyl)piperidine, according to the general aminolysis procedure, afforded **15** (93%), after digestion in dry DMF and trituration with ether, as an amorphous brown powder: mp 237–237.5 °C; IR (KBr) 3450 (br, OH), 3360 (NH), 3140, 3080, 1720 (C=O), 1682 (quinone C=O), 1626, and 1600 cm^{-1}; NMR δ 1.0–1.2 (m, 8 H, NCH_2CH_2CH), 1.35 (t, J = 6.3 Hz, 4 H, CH_2CH_2OH), 1.6–1.7 (m, 2 H, $CHCH_2CH_2OH$), 1.92 (t, J = 11.3 Hz, 8 H, NCH_2CH_2CH), 2.5–2.9 (ABq, 8 H, $COCH_2CH_2$), 3.42 (t, J = 6.3 Hz, 4 H, CH_2OH), 4.35 (m, D_2O removes, 2 H, O*H*), 8.06 (dd, J = 8.6 Hz, J = 2.2 Hz, 2 H, H-3,7), 8.17 (d, J = 8.6 Hz, 2 H, H-4,8), 8.42 (d, J = 2.2 Hz, 2 H, H-1,5), and 10.81 (s, D_2O removes, 2 H, N*H*); MS (rel intensity) m/z 605 ($[M + 1]^{\cdot+}$, 40), 604 ($[M]^{\cdot+}$, 21), 603 ($[M - 1]^{\cdot+}$, 7), 575 ($[M - 1 - C_2H_4]^{\cdot+}$, 4), 495 (23), 461 ($[M - 1 - C_8H_{16}NO]^{\cdot+}$, 10), 391(12) and 369(15). Anal. ($C_{34}H_{44}N_4O_8$) C, H, N. Diacetate salt: mp 203–205 °C dec.

2,6-Bis[3-[4-(2-hydroxyethyl)piperazino]propionamido]anthracene-9,10-dione (16). Compound **3** was treated with 4-(2-hydroxyethyl)piperazine generally according to the method for **5** above, except that reflux was for 14 h and the crude product was digested in DMF prior to treatment with charcoal. Trituration of the filtrate with ether furnished **16** (97%) as a yellow powder: mp 238–239 °C; IR (Nujol) 3380 (br, OH), 3300 (NH), 3200, 3120, 3060, 1708 (C=O), 1670 (quinone C=O), 1620, and 1588 cm^{-1}; NMR δ 2.35 (t, J = 6.3 Hz, 4 H, NCH_2CH_2OH), 2.4–2.5 (m, 16 H, $N(CH_2)_2N$), 2.55–2.65 (ABq, 8 H, $COCH_2CH_2$), 3.47 (t, J = 6.3 Hz, 4 H, CH_2OH), 4.40 (s, 2 H, D_2O removes, O*H*), 8.05 (dd, J = 8.4 Hz, J = 2.0 Hz, 2 H, H-3,7), 8.21 (d, J = 8.4 Hz, 2 H, H-4,8), 8.43 (d, J = 2.0 Hz, 2 H, H-1,5), and 10.75 (s, 2 H, D_2O removes, N*H*); MS (rel intensity) m/z 607 ($[M + 1]^{\cdot+}$, 20), 553 (22), 461 ($[M - 2 - C_7H_{15}N_2O]^{\cdot+}$, 48), 369 (100), 277 (100), 207 ($[C_{14}H_7O_2]^{\cdot+}$, 100), 206 ($[C_{14}H_6O_2]^{\cdot+}$, 11), 171 (100), 143 ($[C_7H_{15}N_2O]^{\cdot+}$, 75), 131 (50), 129 ($[C_6H_{13}N_2O]^{\cdot+}$, 37), and 93 (100). Anal. ($C_{32}H_{42}N_6O_6 \cdot H_2O$) C, H, N. Tetraacetate salt: mp 235–236 °C.

2,6-Bis[3-[bis(2-hydroxyethyl)amino]propionamido]anthracene-9,10-dione (17). Diethanolamine (25.0 g, 0.24 mol) in EtOH (100 mL) was added during 30 min to a stirred, refluxing suspension of amide **3** (8.0 g, 19.1 mmol) in EtOH (150 mL) and

boiling was continued for 22 h. Evaporation of the solvent gave a brown, hygroscopic residue which was digested in 2-propanol (100 mL), triturated with ether (500 mL), and recovered by filtration. After two further such treatments, the solid was washed with ether (3 × 100 mL) and dried. Recrystallization from aqueous EtOH (10% v/v), with charcoal treatment, afforded the amine 17 (9.49 g, 89%) as yellow prisms: mp 159–160 °C; IR (KBr) 3401 (br, OH), 3103 (br, NH), 1685 (C=O), 1672 (quinone C=O), and 1584 cm^{-1}; NMR δ 2.86 (t, J = 6.4 Hz, 4 H, $COCH_2$), 3.11 (t, J = 4.8 Hz, 8 H, CH_2CH_2OH), 3.36 (t, J = 6.4 Hz, 4 H, $COCH_2CH_2$), 3.72 (t, J = 4.8 Hz, 8 H, CH_2OH), 5.36 (s, D_2O removes, 4 H, OH), 8.06 (dd, J = 8.5 Hz, J = 2.1 Hz, 2 H, H-3,7), 8.18 (d, J = 8.5 Hz, 2 H, H-4,8), 8.49 (d, J = 2.1 Hz, 2 H, H-1,5), and 11.00 (s, D_2O removes, 2 H, NH); MS (rel intensity) m/z 557 ($[M + 1]^{\bullet+}$, 30), 452 ($[M - C_4H_{10}NO_2]^{\bullet+}$, 12), 424 ($[M - C_6H_{14}NO_2]^{\bullet+}$, 10), 397 ($[M + 1 - C_7H_{14}NO_3]^{\bullet+}$, 12), 223 (78), 185 (100), 157 (100), 152 (38), and 139 (33); MS (FAB, rel intensity) m/z 557 ($[M + 1]^{\bullet+}$, 38), 429 (4), 277 (5), 215 (5), and 185 (100). Anal. ($C_{28}H_{38}N_4O_8$) C, H, N.

Attempted Synthesis of 2,6-Bis(4-piperidinobutyramido)anthracene-9,10-dione (18). Piperidine (25 mL, 0.25 mol) was added during 15 min to a stirred, refluxing suspension of chlorobutyramide 4 (10.0 g, 22.3 mmol) in EtOH (300 mL). Heating was continued for 110 h, with periodic addition of further portions of piperidine (total 55 mL, 0.55 mol). TLC analysis indicated the presence of amide 4 (ca. 20%) and several polar products. Workup according to the general aminolysis method gave a red-orange solid. Attempted separation of butyramide 18, formed in only <15% yield (HPLC–MS and NMR), from the crude mixture was hampered by poor solubility. Qualitatively similar behavior (ca. 5–20% formation of product) was noted during treatment of chloro amide 4 with morpholine, diethylamine, or 4-methylpiperazine but, in each case, the required products were ultimately difficult to free from associated polar byproducts. Addition of NaI catalyst to the reaction mixture (1–5 g) had little influence upon the progress of aminolysis, while higher-boiling solvents (DMF–EtOH or DMF) led to greater formation of unwanted byproducts.

Preparation of Acetic Acid Addition Salts. General Procedure. A solution of the amino amide (4–6 mmol) in glacial HOAc (30 mL) is heated to 50–60 °C, treated with decolorizing charcoal (500 mg), and filtered. Trituration of the clear filtrate with ether gives a hygroscopic precipitate which is repeatedly digested with dry ether ((3–4) × 100 mL), filtered, washed with further dry ether, and dried in vacuo at 25 °C. The acid addition salts were typically formed as amorphous powders in 75–90% yield.

2,6-Bis[3-(diethylamino)propionamido]anthracene-9,10-dione N,N'-Dimethiodide (19). General Procedure for Preparation of Quaternary Methiodide Salts. A mixture containing amino amide 11 (3.0 mmol), iodomethane (10 mL, 0.16 mol), and acetone (50 mL) is stirred at 25 °C for 24 h. The brown-orange solid which separates is filtered, washed with dry ether (3 × 60 mL), and dried in vacuo at 25 °C. The bis(methylammonium) quaternary methiodide salt 19 is recovered (96%) as an amorphous powder: IR (KBr) 3431 (br, NH), 3099, 3043, 1696 (C=O), 1667 (quinone C=O), 1592, and 1532 cm^{-1}; NMR δ 1.27 (t, J = 7.1 Hz, 12 H, CH_2CH_3), 2.93 (t, J = 7.4 Hz, 4 H, $COCH_2$), 2.98 (s, 6 H, NCH_3), 3.36 (q, J = 7.1 Hz, 8 H, CH_2CH_3), 3.61 (t, J = 7.4 Hz, 4 H, $COCH_2CH_2$), 8.06 (d, J = 8.5 Hz, 2 H, H-3,7), 8.20 (d, J = 8.5 Hz, 2 H, H-4,8), 8.46 (s, 2 H, H-1,5), and 10.79 (s, 2 H, D_2O removes, NH).

X-ray Crystallography. For X-ray crystallography the free base 5 was recrystallized from $CHCl_3$–EtOH (3:2 v/v) to give yellowish-green lath-shape crystals.

Crystal data and conditions for data collection and final R factors are summarized in Table II. Following examination under a light microscope, a single crystal of dimensions 0.4 × 0.05 × 0.02-mm was selected. Preliminary unit cell and space group data was obtained from oscillation and Weissenberg photographs. Intensity data for a unique data set were measured with Ni-filtered Cu K_α radiation (λ = 1.541 78 Å) on an Enraf-Nonius CAD4 automated diffractometer, operated in the $\omega - 2\theta$ mode. A periodic check on the intensities of three strong reflections showed that no significant crystal decay (<1%) or slippage occurred during data collection. The crystal structure was solved by direct methods using the MULTAN82[24] program and refined by full-matrix least-squares techniques minimizing the function $\sum w(F_o - F_c)^2$. The positions of the majority of the hydrogen atoms were found using difference Fourier syntheses; others were generated using standard geometric considerations. All non-hydrogen atoms were refined anisotropically and the positional and thermal parameters of hydrogen atoms were fixed during the refinement in view of the small number of observed reflections. A non-Poisson distribution weighting scheme was used of the form $w = [\sigma^2(F) + (P|F|)^2]^{-1}$, where P (an estimate of experimental uncertainty) was assigned a value of 0.04. Previous crystallographic analyses from this laboratory have found that this value gives a satisfactory weighting scheme as judged by an analysis of agreement between F_c and F_o values. $\sigma(F)$ values were obtained from counting statistics. Refinement was judged to have converged when the shift/error for all parameters was <0.01. This gave a final R factor of 0.0638 and wR of 0.0602. A final difference Fourier synthesis did not show any features of electron density outside the range ±0.2e $Å^{-3}$. All calculations were performed on a VAX 11/750 computer using the Enraf-Nonius SDP package.[25] Table III gives the non-hydrogen atom positional parameters and averaged thermal parameters of 5. As the structure is situated on a crystallographic 2-fold axis, Figure 1 shows the molecular structure of 5 together with its symmetry-related other half. Tables of hydrogen atom coordinates and non-hydrogen atom anisotropic thermal parameters are deposited as supplementary material.

DNA Binding Experiments. Mitoxantrone hydrochloride (Lederle Pharmaceuticals) was obtained from the Royal Marsden Hospital Pharmacy, Sutton, Surrey, UK. Calf thymus DNA (type-I, highly-polymerized sodium salt), *Micrococcus lysodeikticus* DNA and *Clostridium perfringens* DNA were purchased from Sigma Chemical Co., UK. PM2-DNA (cccDNA) was purchased from Boehringer-Mannheim, UK.

The aqueous buffers used were HNE buffer (10 mM HEPES, 1.0 mM EDTA, 10 mM NaCl, pH 7.0, μ = 0.01), MES buffer (2 mM MES, 1.0 mM EDTA, 100–500 mM NH_4F, pH 6.4, μ = 0.1–0.5), and TRIS buffer (50 mM TRIS, 20 mM sodium acetate, 18 mM NaCl, 2.0 mM EDTA, pH 8.0).

Determination of Binding Parameters. The effects of DNA on the UV–visible absorption properties of the acetic acid addition salts of the novel compounds were studied by spectroscopic methods using a Cary 219 spectrophotometer operating at 25.0 ± 0.2 °C. All compounds examined obeyed Beer's law over the range of concentrations used (0–60 μM), and the molar extinction coefficients were determined at their respective visible λ_{max} values.

For the spectroscopic studies, titration of the compounds with calf thymus DNA solution in HNE buffer resulted in precipitation of a partially-soluble complex at high ligand concentrations. This problem was overcome by switching to MES buffer (μ = 0.01–0.1), in which precipitation was not apparent, and this buffer was used for subsequent studies.

Titrations were performed directly in a cuvette by serial addition of 10–20 μL aliquots of a DNA solution (0.6–1.5 mM DNAp in MES buffer) to a solution (2 mL) of compound of known concentration in the same buffer. After thorough mixing, the absorbance at the visible λ_{max} of the ligand was recorded. Titrations were continued until the normalized absorbance, corrected for dilution, was invariant (usually at final DNAp to ligand mole ratios of less than 10:1). The equilibrium free versus bound ligand concentrations, and hence the binding ratio, were calculated by the method of Peacocke and Skerret.[26] Experimental data were plotted using the method of Scatchard and analyzed by the extended neighbor-exclusion model of McGhee and von Hippel.[27]

(24) Main, P.; Hull, S. E.; Lessinger, L.; Germain, G.; DeClercq, J.-P.; Woolfson, M. M. *MULTAN82. A System of Programs for the Automatic Solution of Crystal Structures from X-ray Diffraction Data.* Universities of York and Louvain: York, England, and Louvain, Belgium, 1982.

(25) Frenz, B. A. *Enraf-Nonius SDP Structure Determination Package.* Enraf-Nonius: Delft, The Netherlands, 1985.

(26) Peacock, A. R.; Skerret, J. N. H. The Interaction of Aminoacridines with Nucleic Acids. *Trans. Faraday Soc.* **1956**, *52*, 261–279.

A least-squares fitting procedure was used to derive the binding parameters (K, n, and w), using programs written by one of the authors (T.C.J.).

Thermal Denaturation Studies. Experiments were performed in stoppered quartz cuvettes using a Varian-Cary 219 spectrophometer fitted with a Neslab thermoprogrammer and a circulating water bath. Samples were continuously heated at a rate of 1 °C min^{-1}, in the temperature range of 20–99 °C. The temperature within a proximate filled dummy cuvette was monitored and used to provide chart profiles of optical absorbance at 260 nm versus temperature. A cell programmer accessory, used to position a 5-cell sample turret, was used for multiple sampling. The melting profiles were digitized and the transition melting temperature (T_m) was determined at the midpoint of the normalized curves;[28] results are given as the mean from at least three determinations.

All DNA samples were dissolved in HNE buffer and purified by extensive dialysis and centrifugation prior to use. For studies with calf thymus DNA, where the DNAp concentration was fixed at 0.10 mM, DNA to ligand mole ratios of 40:1, 20:1, and 10:1 were examined, using HNE-buffered solutions (pH 7.0). In the case of *M. lysodeikticus* and *C. perfringens* DNAs, the working DNAp and ligand concentrations were 0.10 and 0.01 mM, respectively, giving a DNAp to ligand ratio of 10:1. The six compounds examined in this study, containing either diethylamine or piperidine functions, were chosen to assess the possible effects of side-chain length, steric bulk, and the inclusion of hydroxyl groups upon DNA binding.

Where appropriate, 1% v/v DMSO was used in the dissolution of compounds of poor aqueous solubility. It was established that this cosolvent had no significant effect upon the T_m of either the native DNA or the DNA–ligand complex. Further, the T_m values for the free base, where soluble, and acetate salt forms of the agents were shown to differ by <0.2 °C.

Unwinding of PM2-DNA. Electrophoretic titrations were carried out according to the procedure of Espejo and Lebowitz,[29] using bacteriophage pM2-DNA as a source of cccDNA. The DNA was dissolved in TRIS buffer (10 mM TRIS-HCl, 1 mM EDTA, pH 8.0). Agarose gels (1.2% w/w in TRIS buffer) were loaded with the DNA solution (200 ng of DNAp) containing the added compound, such as to provide a range of DNAp to ligand molar ratios, together with loading buffer (7% w/w sucrose). Electrophoresis (60 V, 3.5 mA at 20 °C) was performed for 2–3 h; gels were then extruded, stained with ethidium bromide, and photographed using UV transillumination (Polaroid film type 55). Ethidium bromide was used as a control compound, and berenil was used to verify that a DNA groove-binding ligand would not produce the same effects upon cccDNA as a known DNA intercalator.[30]

The critical free drug concentration (c') for each agent was estimated as that at which cccDNA most nearly co-migrates with "nickel" DNA in the sample. Unwinding angles (ϕ) were calculated using a ϕ-value of 26° for the ethidium bromide control, a superhelical density of −0.091 for pM2-DNA, and a value of 0.063 for r', the critical molar binding ratio, quoted for ethidium bromide[29] to derive the equation:

$$\phi = 1.638/r'$$

This equation was used to calculate the unwinding angles in Table VI, by using the binding parameters and r' calculated from the determined c' values.

Molecular Modeling. This study involved the use of a consensus dinucleoside intercalation site geometry d(CpG) initially derived from the crystal structure of a dinucleoside phosphate d(CpG)–proflavine intercalation complex.[31] The (CpG) intercalation site was contained in the center of an alternating hexanucleotide duplex of sequence d(5′-TACGTA-3′). This hexamer sequence was itself derived from a decanucleotide complex, constructed by means of least-squares fitting of B-form DNA residues to both ends of the d(CpG) dinucleoside intercalation geometry found in the d(CpG)–proflavine crystal structure, followed by energy minimization.[32] The two terminal base pairs at each end of the decanucleotide sequence were deleted to give the hexamer sequence used in the modeling studies. This was done in order to save computer time. Initial studies showed no advantage using a decanucleotide model since all the compounds examined have binding sites smaller than hexanucleotides.

Coordinates for the chromophore and the amide portion of the side chain for each ligand were taken from the crystal structure of **5**. Alternative side chains were generated by computer graphics modeling; all had a proton located on the amine nitrogen atoms (to simulate their protonated state in solution conditions). With **7**, **11**, and **17**, the flexible terminal amine moieties were positioned so as to minimize contact between the alkyl hydrogen atoms. This was judged to be at separations of ≥2.1 Å, achieved by rotation of appropriate torsion angles between the nitrogen, carbon, and hydrogen atoms of the amine group. These operations were performed on a Silicon Graphics IRIS4D-20G workstation using the molecular modeling program GEMINI.[33] Partial atomic charges (MNDO) for the diprotonated compounds molecules in their intercalated conformations were calculated using the AMPAC program.[34]

Interactive graphics modeling using GEMINI was used to dock the molecules into the d(CpG) intercalation site of the hexamer duplex with acceptable nonbonded contacts. The dinucleotides at this site were held fixed during such maneuvres.

The starting intercalated position of the chromophore was the same for all the $n = 2$ compounds to ensure that the differences obtained for the energy-minimized complexes were due to the side-chain substitutions. The same procedure was used for the $n = 1$ compounds, but with a different chromophore starting position due to steric clashes with the DNA backbone resulting from the inflexibility of the shorter side chains. In general, better overlap between the base pairs at the intercalation site and the chromophore was achieved with the $n = 2$ derivatives, with the chromophore positioned almost parallel to the long axis of the base pairs. With the $n = 1$ derivatives, parallel positioning of the chromophore resulted in repulsive contacts with the DNA backbone, which could not be relieved due to the relative inflexibility of the shorter side chain. These derivatives were thus intercalated diagonally between the long axes of the base pairs. With both the $n = 1$ and 2 derivatives, the side-chain amide groups were positioned with the NH oriented toward the sugar–phosphate backbone and the carbonyl directed into the groove. The conformations of the side chains were optimized on the graphics systematically altering all their torsion angles.

The resulting DNA–ligand intercalated complexes were subjected to molecular mechanics all-atom energy minimization. The force-field parameters used for the DNA were an all-atom rep-

(27) McGhee, J. D.; von Hippel, P. H. Theoretical Aspects of DNA-Protein Interactions: Co-operative and Non-co-operative Binding of Large Ligands to a One-Dimensional Homogeneous Lattice. *J. Mol. Biol.* **1974**, *86*, 469–489.

(28) Jones, G. B.; Davey, C. L.; Jenkins, T. C.; Kamal, A.; Kneale, G. G.; Neidle, S.; Webster, G. D.; Thurston, D. E. The Non-Covalent Interactions of Pyrrolo[2,1-c][1,4-benzodiazepine-5,11-diones with DNA. *Anti-Cancer Drug Des.* **1990**, *5*, 249–264.

(29) Espejo, R. T.; Lebowitz, J. A Simple Electrophoretic Method for the Determination of Superhelix Density of Closed Circular DNAs and for Observation of their Superhelix Density Heterogeneity. *Anal. Biochem.* **1976**, *72*, 95–103.

(30) Waring, M. J. Variation of the Supercoils in Closed Circular DNA by Binding of Antibiotics and Drugs: Evidence for Molecular Models Involving Intercalation. *J. Mol. Biol.* **1970**, *54*, 247–279.

(31) Shieh, H.-S.; Berman, H. M.; Dabrow, M.; Neidle, S. The Structure of Drug-Deoxydinucleoside Phosphate Complex; Generalised Conformational Behaviour of Intercalation Complexes with RNA and DNA Fragments. *Nucleic Acids Res.* **1980**, *8*, 85–96.

(32) Neidle, S.; Pearl, L. H.; Herzyk, P.; Berman, H. M. A Molecular Model for Proflavine-DNA Intercalation. *Nucleic Acids Res.* **1988**, *16*, 8999.

(33) Beveridge, A. J. *GEMINI, version 1.03, a molecular modelling program for Silicon Graphics workstations.* Available from the CRC Biomolecular Structure Unit, The Institute of Cancer Research, Sutton, Surrey SM2 5NG, UK.

(34) QCPE Program 506, Dept. of Chemistry, Indiana University, IN 47405.

resentation;[35,36] parameters for the drug molecules were developed in previous studies in this laboratory. A distance-dependent dielectric constant of the form $\epsilon = 4r_{ij}$ was used.[37] The energy minimization calculations were performed using the EMPMDS program[38] on a VAX 11/750 computer. Refinements for the DNA–ligand complexes, and the separate DNA and ligands, were judged to have reached convergence in total energy when the rms value of the first derivative was ≤0.15 kcal mol^{-1} Å^{-1}. This was achieved within approximately 2000 cycles of energy refinement.

Biological Activity in Vitro. Three cell lines, leukemia L1210, Walker 256 (WS) carcinoma, and V79 Chinese hamster ovarian, were used. In each case, cells at a density of ca. 5×10^3 cells mL^{-1} were grown for 24 h, counted to confirm logarithmic growth, and treated with the compound (as the acetic acid addition salt or free base forms for 5–17) in aqueous solution. Incubation was continued for 2 days for the L1210 and WS assays and 6 days for the V79 cells. The surviving cells were then counted and the percentage inhibition in growth was calculated as compared to untreated controls.

Acknowledgment. We thank Mr. M. Baker for obtaining mass spectra, Mrs. P. M. Goddard and M. Valenti for in vitro and in vivo screening of all compounds, and Dr. A. Beveridge for assistance with early aspects of the molecular modeling. This work was supported by the Cancer Research Campaign.

Supplementary Material Available: Tables of hydrogen atom coordinates and non-hydrogen atom anisotropic thermal parameters (2 pages). Ordering information is given on any current masthead page.

(35) Weiner, S. J.; Kollman, P. A.; Case, D. A.; Singh, U. C.; Ghio, C.; Alagona, G.; Profeta, S.; Weiner, P. A New Force Field for Molecular Mechanical Simulation of Nucleic Acids and Proteins. *J. Am. Chem. Soc.* **1984**, *106*, 765–784.
(36) Weiner, S. J.; Kollman, P. A.; Nguyen, D. T.; Case, D. A. An All-Atom Force Field for Simulations of Proteins and Nucleic Acids. *J. Comput. Chem.* **1986**, *7*, 230–252.
(37) Orozco, M.; Laughton, C. A.; Herzyk, P.; Neidle, S. Molecular-Mechanics Modelling of Drug-DNA Structures; The Effects of Differing Dielectric Treatment on Helix Parameters and Comparison with a Fully Solvated Structural Model. *J. Biomol. Struct. Dyn.* **1990**, *8*, 359–374.
(38) Haneef, I. Ph.D. Thesis, University of London, 1985.

Syntheses, Resolution, and Structure–Activity Relationships of Potent Acetylcholinesterase Inhibitors: 8-Carbaphysostigmine Analogues

Yuhpyng L. Chen,* Jann Nielsen, Kirk Hedberg, Audrey Dunaiskis, Shawn Jones, Lorena Russo, Jonathan Johnson, Jeffrey Ives, and Dane Liston

Medicinal Chemistry and Neuroscience Departments, Central Research Division, Pfizer Inc., Groton, Connecticut 06340.
Received August 2, 1991

The synthesis of a series of 1,2,3,3a,8,8a-hexahydroindeno[2,1-*b*]pyrrole 5-alkylcarbamates and their resolution are reported. These compounds are structurally related to physostigmine with substitution of a methylene group in place of the NMe group at position 8 of physostigmine. Many of these 8-carbaphysostigmine analogues are more potent acetylcholinesterase inhibitors in vitro and less toxic in vivo than physostigmine. The (−)-enantiomer (e.g., **1d** and **1g**) possessing the same absolute configuration at C_{3a} and C_{8a} as that of physostigmine, is about 6 to 12-fold more potent at inhibiting acetylcholinesterase than the corresponding (+)-enantiomer (e.g., **1e** and **1h**).

Clinical studies suggest that acetylcholinesterase (AChE) inhibitors, such as THA (tetrahydro-9-aminoacridine) and physostigmine, may be useful in enhancing memory in patients with Alzheimer's disease.[1–4] However, THA induces a high incidence of liver toxicity.[5] The liver toxicity produced by THA may be structure-dependent rather than mechanism-related since physostigmine reportedly has not produced liver toxicity in clinical trials.[6,7] Physostigmine suffers from a short half-life, variable bioavailability, and a narrow therapeutic index,[8] which may account for the inconsistent clinical efficacy. A controlled-release formulation of physostigmine (Cogmine) is currently in phase III clinical trials for the treatment of Alzheimer's disease.[6] The related analogue, heptylphysostigmine (MF-201), was reported to have significantly less toxicity than physostigmine while retaining its in vitro potency in inhibiting AChE.[7] We envisioned replacing the *N*-methyl group at N_8 of the physostigmine nucleus with a methylene group to increase its chemical and metabolic stability by modification of the less stable aminal group to a more stable amino group. Since the cationic protonated amine at N_1 of physostigmine interacts with the anionic site of AChE, the resulting structure, 8-carbaphysostigmine **1**, would be expected to show better interaction with the enzyme because of its increased basicity. Furthermore, modifications

(1) Summers, W. K.; Majovski, L. V.; Marsh, G. M.; Tachiki, K.; Kling, A. Oral Tetrahydroaminoacridine in Long-term Treatment of Senile Dementia, Alzheimer Type. *N. Engl. J. Med.* **1986**, *315*, 1241.
(2) Becker, R. E.; Giacobini, E. Mechanisms of Cholinesterase Inhibition in Senile Dementia of the Alzheimer Type: Clinical, Pharmacological, and Therapeutic Aspects. *Drug Dev. Res.* **1988**, *12*, 163.
(3) Davis, K. L.; Mohs, R. L.; Tinklenberg, J. R. Enhancement of Memory by Physostigmine. Letters to the Editor. *N. Engl. J. Med.* **1979**, *300*, 946.
(4) Kumar, V.; Calache, M. Treatment of Alzheimer's Disease with Cholinergic Drugs. *Int. J. Clin. Pharmacol., Ther. Toxicol.* **1991**, *29*, 23.
(5) Marx, J. T. Alzheimer's Drug Trial Put on Hold. *Science* **1987**, *238*, 1041.
(6) *Script* **1989**, July 19, p 11.
(7) Brufani, M.; Maurizio, M.; Pomponi, M. Anticholinesterase Activity of a New Carbamate, Heptylphysostigmine, in View of Its Use in Patients with Alzheimer-type Dementia. *Eur. J. Biochem.* **1986**, *157*, 115.
(8) Thal, L. T.; Fuld, P. A. Memory Enhancement with Oral Physostigmine in Alzheimer's Disease. *N. Engl. J. Med.* **1983**, *308*, 720.

0022-2623/92/1835-1429$03.00/0 © 1992 American Chemical Society